Journal of Organometallic Chemistry, 362 (1989) 105–115
Elsevier Sequoia S.A., Lausanne – Printed in The Netherlands

A multinuclear (^{1}H, ^{13}C and ^{95}Mo) NMR investigation of sulphur inversion in molybdenum tetracarbonyl complexes of chelating dithioethers

Edward W. Abel, David E. Budgen, Ian Moss, Keith G. Orrell and Vladimir Šik
Department of Chemistry, The University, Stocker Road, Exeter EX4 4QD (Great Britain)

(Received July 4th, 1988)

Abstract

The complexes *cis*-[$Mo(CO)_4(RSCH_2CH_2SR)$] (R = Me, Et, ^{i}Pr, ^{t}Bu); *cis*-[$Mo(CO)_4$(*cis*-$^{t}BuSCH{=}CHSBu^{t}$)] and *cis*-[$Mo(CO)_4(MeSCH_2CH_2SBu^{t})$] have been prepared, and the pyramidal sulphur inversion investigated by variable temperature ^{1}H and $^{13}C\{^{1}H\}$ NMR spectroscopy, and variable temperature ^{1}H 2D NMR exchange spectroscopy. Sulphur inversion barriers calculated for these complexes show a marked dependence on the steric requirements of the dithioether ligand. Molybdenum-95 NMR chemical shifts have been rationalised in terms of the relative strengths of molybdenum–sulphur bonding, and qualitatively correlated with the sulphur inversion barriers.

Introduction

Pyramidal sulphur inversion in transition metal complexes has been investigated extensively in recent years, and accurate inversion barriers have been calculated in many cases by bandshape analysis [1] of variable temperature NMR spectra, or, more recently, from quantitative two-dimensional exchange spectroscopy (EXSY) [2]. Many of the factors that influence the magnitude of these inversion barriers are now understood [3]. We have recently employed variable temperature 1D and 2D NMR spectroscopy to investigate the effect of substituents of varying steric requirements at the inverting sulphur centre in transition metal complexes of dithioethers, including group 6 metal tetracarbonyl [4] and trimethylplatinum(IV) halide [5,6] derivatives. These studies have revealed a marked dependence of the sulphur inversion barriers on the steric requirements of the dithioethers, with the free energy of activation $\Delta G^{\ddagger}$(298 K) decreasing with increasing steric demand of the ligand.

The magnitude of the barrier to sulphur inversion in a transition metal complex is a reflection of the strength of the metal–sulphur bonding [3]. Thus, for example, the marked differences in inversion barriers observed for *cis*-[$PtCl_2(SEt_2)_2$] ($\Delta G^{\ddagger}$

0022-328X/89/$03.50

70.3 kJ mol^{-1}) and *trans*-[$PtCl_2(SEt_2)_2$] ($\Delta G^{\ddagger}$ 58.2 kJ mol^{-1}) [7] are a consequence of the greater *trans*-influence of SEt_2 relative to Cl and the resultant weakening of the metal–sulphur bond. Molybdenum-95 NMR chemical shifts have been shown to be highly sensitive to structural and electronic variations within a series of closely related compounds [8]. For example, in the series of compounds [(arene)$Mo(CO)_3$], where arene = toluene, *o*-xylene, *m*-xylene, *p*-xylene and mesitylene, shielding of the ^{95}Mo nucleus increases in the order mesitylene > *m*-xylene > *p*-xylene > *o*-xylene > toluene [9], which may be correlated with the concomitant weakening of the metal–arene bonding. Since therefore, the strength of molybdenum–sulphur bonding would be expected to influence both barriers to sulphur inversion and values of $\delta(^{95}Mo)$ in sulphur-containing molybdenum complexes, we have prepared a range of complexes of the type *cis*-[$Mo(CO)_4L$], where L represents a series of chelating dithioether ligands with varying steric requirements. The complexes studied were *cis*-[$Mo(CO)_4(RSCH_2CH_2SR)$] (R = Me (**1**), Et (**2**), ^{i}Pr (**3**) and ^{t}Bu (**4**), *cis*-[$Mo(CO)_4$(*cis*-^{t}BuSCH=CHSBu^{t})] (**5**) and *cis*-[$Mo(CO)_4(MeSCH_2CH_2SBu^{t})$] (**6**). Where possible, both sulphur inversion barriers and ^{95}Mo chemical shifts have been evaluated in order to assess the extent of correlation between these two sets of parameters. The ^{95}Mo NMR results also serve to extend the limited range of chemical shift data available for molybdenum(0) complexes of sulphur-coordinated ligands [10,11].

Experimental

General

All preparations were performed under dry nitrogen by standard Schlenk techniques [12]. Toluene and hexane were dried over sodium and distilled from sodium diphenyl ketyl under nitrogen prior to use. Dichloromethane was dried over calcium hydride and distilled under nitrogen prior to use. The ligand $EtSCH_2CH_2SEt$ was purchased from K & K Chemicals and used without further purification. The ligands $MeSCH_2CH_2SMe$ [13], $^{i}PrSCH_2CH_2SPr^{i}$ [13] and $MeSCH_2CH_2SBu^{t}$ [6] were prepared by published methods. Infrared spectra were recorded in CH_2Cl_2 solution on a Perkin–Elmer 398 spectrometer interfaced to a Perkin–Elmer 3600 Data Station, and were calibrated by use of the 1602 cm^{-1} signal of polystyrene. Elemental analyses were performed by Butterworth Laboratories Ltd., London.

Preparations of the complexes

The complexes **1**, **2**, **3** and **6** were prepared by a published method by direct thermal reaction of [$Mo(CO)_6$] with the appropriate ligand in refluxing toluene [14,15]. Yields, melting points and infrared and analytical data are given in Table 1. The syntheses of **4** and **5** have been reported previously [4].

NMR studies

Hydrogen-1, $^{13}C\{^{1}H\}$ and ^{95}Mo NMR spectra were recorded on a Bruker AM-250 FT NMR spectrometer operating at 250.13 MHz (^{1}H), 62.90 MHz (^{13}C) and 16.28 MHz (^{95}Mo). A standard variable temperature unit was used to control the probe temperature, and temperatures are considered accurate to $\pm 1°C$.

Two-dimensional ^{1}H EXSY spectra for **1** were obtained using the Bruker automation program NOESY, using a mixing time τ_m of 0.1–0.3 s. The F_1 data table

Table 1

Synthetic, analytical and infrared data for complexes **1–3** and **6**

Complex	Yield (%) [a]	ν(CO) (cm^{-1}) [b]	Analytical data (Found (Calcd.) (%))		Melting point (°C) [c]
			C	H	
1	28.8	2016(m), 1911(vs,br), 1861(s)	29.0 (29.1)	3.1 (3.1)	152–160(d)
2	57.5	2016(m), 1911(vs,br), 1860(s)	33.4 (33.5)	3.9 (3.9)	114–115
3	72.5	2016(m), 1905(vs,br), 1856(s)	37.3 (37.3)	4.9 (4.9)	76– 77
6	76.9	2030(m), 1915(vs), 1899(vs), 1865(m)	35.8 (35.5)	4.5 (4.3)	110–111

[a] Relative to $[Mo(CO)_6]$. [b] Recorded in CH_2Cl_2 solution. [c] Uncorrected. d = decomposition.

contained 64 words and was zero-filled to 512 words. The F_2 domain contained 1024 words [2].

Band-shape analyses of the variable temperature 1D NMR spectra were performed using the authors' modified version of the DNMR program of Kleier and Binsch [1,16]. Rate constants for sulphur inversion in **1** were calculated from the 2D NMR signal intensities using the previously described D2DNMR program [2].

All spectra, unless otherwise stated, were recorded in CD_2Cl_2 solution, and chemical shifts are quoted relative to either Me_4Si (^1H, ^{13}C) or aqueous, 2M Na_2MoO_4 solution at pH 11 (^{95}Mo).

Results and discussion

The complexes **1** to **6** were conveniently prepared as described above, and isolated as yellow, air-stable crystalline solids which gave satisfactory elemental analyses and infrared spectra. The complexes **1** [14], **2** [17], **4** [4,15] and **5** [4] have previously been reported.

Variable temperature ^1H and $^{13}C\{^1H\}$ NMR spectra of 1–6

Hydrogen-1 and $^{13}C\{^1H\}$ data for complexes **1–3** and **6** (at ca. −90 °C and at ca. 20 °C) are presented in Tables 2 and 3. Similar data for complexes **4** and **5** have been reported previously [4].

Single-site sulphur inversion in complexes **1–5** proceeds according to the pathways shown in Fig. 1, and involves the interconversion of two DL invertomers and two degenerate *meso* invertomers. However, the two DL invertomers are enantiomeric, and thus only two sets of NMR signals would be expected at temperatures where sulphur inversion is slow on the NMR timescale. For complexes **1–4**, the ^1H and $^{13}C\{^1H\}$ NMR spectra at −90 °C showed features consistent with the presence of these invertomers, and were very similar in form to those recorded for the analogous tungsten complexes [4]. The populations of these invertomers were unequal, and showed a small dependence on the steric bulk of the thioalkyl group. Typically the DL/*meso* ratio was approximately 2/1 which accords with the observation from molecular models that non-bonded interactions between the thioalkyl groups are reduced in the DL invertomer relative to the *meso* invertomer.

Table 2

^{1}H NMR parameters for complexes **1–3** and **6**

(Abbreviations employed are: (s) = singlet; (d) = doublet; (t) = triplet, (q) quartet)

Complex	Temperature (°C)	Chemical shifts and spin–spin coupling constants [a]		
		Methyl protons	Backbone methylene protons	Alkyl group methylene/ methine protons
1	−90	2.37 (s) (DL)	2.72–2.90 (*meso*) [b]	
		2.55 (s) (*meso*)	3.17 (d), 2.46 (d) [10.40] (DL)	
	20	2.42 (s)	2.76 (s)	
2	−90	1.35 (t) [7.07] (DL)	2.60–3.00 (*meso*) [b]	2.54 (q) [7.36] (*meso*) [c]
		1.41 (t) [7.22] (*meso*)	3.30 (d), 2.35 (d) [10.62] (DL)	2.75 (q) [6.93] (DL) [c]
	20	1.37 (t) [7.39]	2.75 (s)	2.71 (q) [7.39] [c]
3	−90	1.40 (d) [6.20] (DL)	2.70–3.00 (*meso*) [b,d]	2.70–3.00 [d,e]
		1.45 (d) [7.08] (*meso*)	3.23 (d) 2.34 (d) [10.84] (DL)	
	20	1.40 (d) [6.62]	2.74 (s)	2.88 [6.62] (septet) [e]
6	−90	1.39 (s) (*syn*) [f]	2.50–3.50 [h]	
		1.47 (s) (*anti*) [f]		
		2.44 (s) (*syn*) [g]		
		2.37 (s) (*anti*) [g]		
	20	1.43 (s) [f]	2.75 (s)	
		2.41 (s) [g]		

[a] Chemical shifts (δ) and spin–spin coupling constants (in parentheses) (^3J(HH) (Hz)). [b] AA'BB' multiplet. [c] Methylene protons. [d] Complete assignment not possible due to signal overlap. [e] Methine protons. [f] $(CH_3)_3CS$. [g] CH_3S. [h] Complex overlapping multiplets observed for both invertomers.

We have previously reported [4] that complex **5** exists in solution exclusively as the *meso* invertomer in marked contrast to the complexes **1–4**. The unsaturated ligand backbone constrains the chelate ring to a planar geometry, and models show

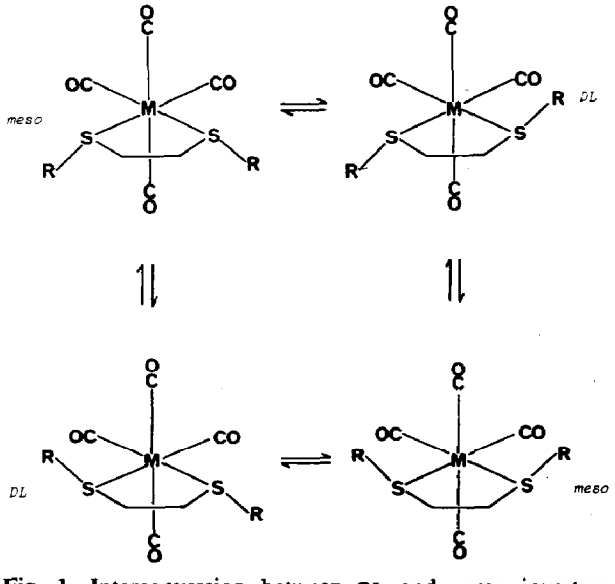

Fig. 1. Interconversion between DL and *meso* invertomers of *cis*-[Mo(CO)$_4$(RSCH$_2$CH$_2$SR)] via single-site sulphur inversion.

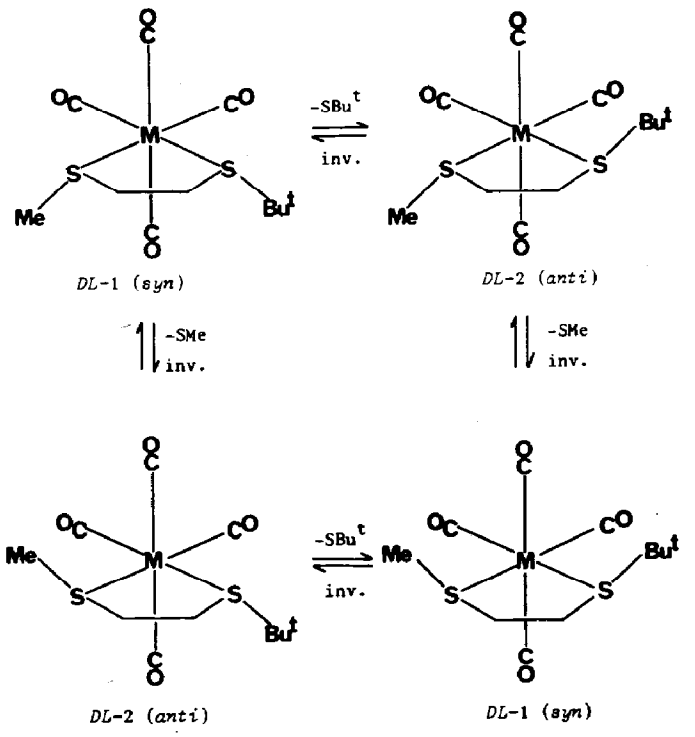

Fig. 2. Interconversion between DL-1 (*syn*) and DL-2 (*anti*) invertomers of *cis*-[$Mo(CO)_4(MeSCH_2CH_2SBu^t)$] via single-site sulphur inversion.

that this results in much larger non-bonded interactions between the t-butyl groups and the axial carbonyl ligands than occurs with the saturated ligands, and furthermore, these interactions are much more severe for the DL invertomer than for the *meso* invertomer.

Single-site sulphur inversion in **6** would be expected to proceed in an analogous manner to the symmetrical ligand complexes **1–4**; however, as a result of the unsymmetrical nature of the ligand, inversion would involve interconversion of two pairs of enantiomeric DL invertomers (Fig. 2). Two sets of signals are therefore expected and were indeed observed in the low temperature ^1H and $^{13}C\{^1H\}$ NMR spectra of **6**, consistent with the presence of both *syn* and *anti* invertomers. In its ^1H NMR spectrum, individual resonances were observed for the two invertomers in both the $SC(CH_3)_3$ and SCH_3 regions of the spectra (Table 2). The methylene region was extremely complex as each invertomer would be expected to give rise to an ABCD multiplet and no analysis was attempted.

The low temperature $^{13}C\{^1H\}$ NMR spectrum of **6** was also consistent with the presence of *syn* and *anti* invertomers (Table 3). The carbonyl region of the spectrum exhibited eight resonances, four (two equatorial and two axial) for each invertomer (Fig. 3). Assignment of the signals in both the ^1H and $^{13}C\{^1H\}$ low temperature spectra for **6** were based on the assumption that the *anti* invertomer slightly predominated in solution. The invertomer population ratio was, in fact, 52/48. This very slight population difference casts some uncertainty on the assignments of the axial CO signals (Table 3) and made it impossible to arrive at a firm assignment of the closely grouped equatorial CO signals.

TABLE 3

$^{13}C\{^1H\}$ NMR parameters for complexes **1–3** and **6**

Complex	Temperature (°C)	Chemical shift (δ)				
		Methyl carbons	Ligand backbone carbons	Alkyl group carbons	Axial carbonyl carbons	Equatorial carbonyl carbons
1	−90	24.69 (DL)	33.63 (DL)		206.26 (DL) [a]	217.91 (DL)
		26.09 (*meso*)	35.98 (*meso*)			218.09 (*meso*)
	20	25.46	35.58		206.67	217.74
2	−90	13.83 (DL)	31.75 (DL)	34.43 (DL) [b]	206.27 (DL)	217.76 (DL)
		14.29 (*meso*)	33.86 (*meso*)	36.53 (*meso*) [b]	205.28, 207.28 (*meso*)	218.03 (*meso*)
	30	13.85	33.51	35.88 [b]	206.72	217.71
3	−90	22.10, 22.39 (DL) [c]	31.34 (DL)	41.42 (DL) [d]	204.49 (DL)	217.98 (DL)
		22.39, 22.58 (*meso*) [c]	32.66 (*meso*)	43.71 (*meso*) [d]	204.85, 207.98 (*meso*)	218.14 (*meso*)
	20	22.43	32.72	42.91 [d]	207.05	217.95
6	−100	25.66 [e,f]	28.80 (*syn*) [h]	48.89 (*syn*) [j]	205.59, 208.46 (*syn*)	218.23 [k], 218.34 [k],
		29.79 (*syn*) [g]	28.37 (*anti*) [h]	48.64 (*anti*) [j]	205.10, 209.10 (*anti*)	218.42 [k], 218.92 [k]
		29.90 (*anti*) [g]	36.49 (*syn*) [i]			
			38.20 (*anti*) [i]			
	20	25.39 [e]	29.49 [h]	48.47 [j]	207.15	217.84 [l], 218.28 [m]
		29.83 [g]	37.73 [i]			

[a] Signals for *meso* invertomer not observed. [b] Methylene carbons. [c] Prochiral methyl groups. [d] Methine carbons. [e] CH_3S. [f] Individual resonances for the two invertomers not observed. [g] $(CH_3)_3CS$. [h] $(CH_3)_3CSCH_2$. [i] CH_3SCH_2. [j] Quaternary carbon. [k] Complete assignment of this region not attempted. [l] *trans* to CH_3S. [m] *trans* to $(CH_3)_3CS$.

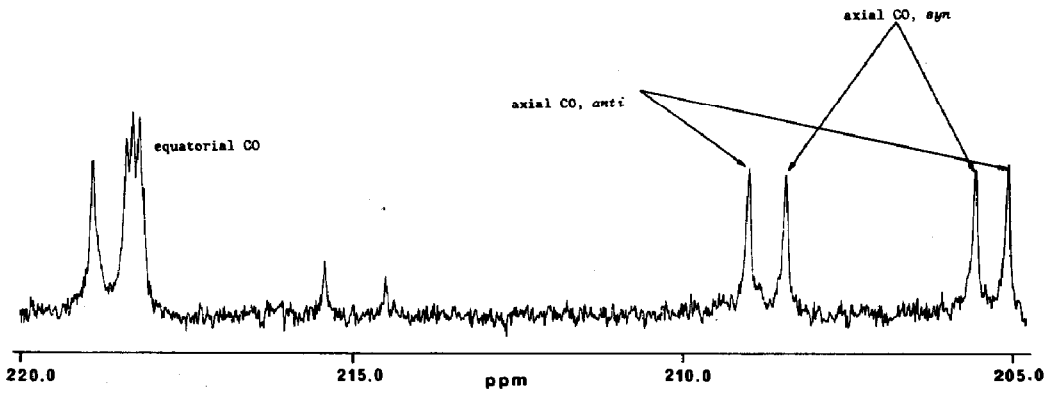

Fig. 3. Carbonyl region of $^{13}C\{^1H\}$ NMR spectrum of **6** in CD_2Cl_2 at $-100\,^\circ C$.

When solutions of **1–6** were warmed, coalescence of signals in all regions of both the ^1H and $^{13}C\{^1H\}$ NMR spectra occurred, until at ambient temperature averaged spectra, consistent with the rapid interconversion of invertomers via sulphur inversion, were observed (Tables 2 and 3). In the case of complex **6**, the nature of the ligand should, in principle, give rise to two separate sulphur inversion processes of widely different activation energies, at each sulphur centre. However, owing to the high symmetry of the $Mo(CO)_4$ moiety, only the faster inversion (considered to be SBu^t inversion [4]) may be observed, as this alone would interconvert *syn* and *anti* invertomers.

Evaluation of activation parameters for sulphur inversion in complexes 1–4

Computer simulations of the methylene region of the $^{13}C\{^1H\}$ variable temperature NMR spectra of complex **2** were performed using the static parameters noted in Table 4, the spin problem being a simple two-site exchange

$$A(\text{DL}) \rightleftharpoons B(meso)$$

For complex **3**, the simulations were performed on the methine region of the $^{13}C\{^1H\}$ spectra due to the slightly larger chemical shift difference between the signals for the two invertomers in this region. Static parameters are again listed in Table 4.

Complex **1** was insufficiently soluble for recording of high quality, variable temperature $^{13}C\{^1H\}$ spectra, suitable for simulation; additionally overlap of the methyl and methylene signals in the variable temperature ^1H spectra precluded

Table 4

Static parameters used in the calculation of pyramidal sulphur inversion energies for complexes **2** and **3**

Complex	Temperature (°C)	ν_A [a] (Hz)	p_A	ν_B [b] (Hz)	p_B	T_2^* (s)
2	−70 [c]	2012.8	0.760	2133.0	0.240	0.094
	−70 [d]	2175.3	0.760	2298.0	0.240	0.094
3	−80 [e]	2606.9	0.680	2741.9	0.320	0.079

[a] DL invertomer. [b] *meso* invertomer. [c] Data for backbone methylene carbons. [d] Data for ethyl group methylene carbons. [e] Data for methine carbons.

Table 5

Rate constants for DL → *meso* exchange via sulphur inversion derived from ^{1}H NMR EXSY experiments for **1**

Temperature (°C)	Mixing time τ_m (s)	Rate constant k (s^{-1})
−75	0.3	0.135
−70	0.2	0.288
−65	0.1	0.636
−60	0.1	1.430

accurate simulation of these bandshapes. Rate constants were, however, obtained for sulphur inversion in **1** using variable temperature two-dimensional ^{1}H EXSY spectroscopy [2]. Rate constants were obtained from the experimental cross-peak intensities using the D2DNMR program [2]. Even with this technique, however, only a limited range of rate constants could be obtained, since below −75 °C it proved impossible to obtain good quality 2D EXSY spectra owing to the poor solubility of **1**, whilst above −60 °C exchange broadening of the methyl signals became significant. The rates obtained are noted in Table 5, and a typical spectrum is shown in Fig. 4.

The rate constants obtained by these methods were used to evaluate Arrhenius and Eyring activation parameters for sulphur inversion in complexes **1**–**3**, and these are listed in Table 6 together with those previously calculated for **4** [4]. The free energies of activation, $\Delta G^{\ddagger}$(298 K), show a marked dependence on the size of the thioalkyl group, varying from 50.0 kJ mol^{-1} for **1** to 40.3 kJ mol^{-1} for **4**. This trend

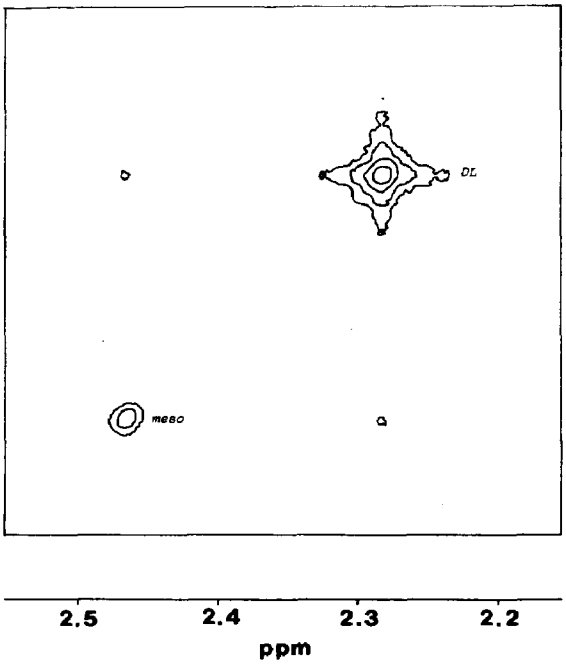

Fig. 4. 2D EXSY spectrum of **1** in CD_2Cl_2 at −70 °C (methyl region).

Table 6

Arrhenius and Eyring activation parameters for pyramidal sulphur inversion for complexes **1–4**

Complex	E_a (kJ mol^{-1})	$\log_{10}$ (A) (s^{-1})	$\Delta H^{\ddagger}$ (kJ mol^{-1})	$\Delta S^{\ddagger}$ (J K^{-1} mol^{-1})	$\Delta G^{\ddagger}$(298 K) (kJ mol^{-1})
1	55.17 ± 1.44	13.67 ± 0.37	53.46 ± 1.42	11.6 ± 6.9	50.00 ± 0.64
2	54.84 ± 0.32	14.22 ± 0.07	52.91 ± 0.33	21.0 ± 1.4	46.64 ± 0.09
3	52.23 ± 0.79	14.41 ± 0.10	50.36 ± 0.42	25.0 ± 1.9	42.91 ± 0.14
4 [a]	46.63 ± 0.79	13.89 ± 0.20	44.89 ± 0.77	15.6 ± 3.7	40.25 ± 0.33

[a] From ref. 4.

is similar to that observed for the related tungsten complexes [4], and may be attributed to the considerable distortion towards a planar sulphur geometry that occurs on increasing the size of the thioalkyl group, thus allowing easier access to the planar transition state that pertains during sulphur inversion [4,6].

As previously noted, the observation of only one invertomer at the slow inversion limit for complex **5** meant that the inversion barrier could only have been evaluated either by 1D bandshape fitting or 2D-EXSY analysis of the axial CO region of the variable temperature $^{13}C\{^1H\}$ NMR spectra. In order to obtain good quality spectra for quantitative studies, a ^{13}CO enriched complex would have been required. It was not felt that the information to be gained from this procedure warranted the preparation of an enriched sample, since the effects of introducing unsaturation into a ligand backbone on sulphur inversion barriers are already well documented [3]. Additionally, quantitative studies on sulphur inversion in **6** were not performed, since it would only have been possible to evaluate the barrier to inversion at SBu^t, which was likely to be very similar to that observed in **4** [6], and which would have led to a misleading result when correlated with ^{95}Mo NMR chemical shifts (see later).

Molybdenum-95 NMR studies

Molybdenum-95 NMR spectra were recorded at ambient temperatures for complexes **1–6**, and the chemical shifts and line widths of the signals are noted in Table 7. Spectra of good quality were generally obtained after 300–500 scans, and linewidths for the signals fell in the range 80–210 Hz. Attempts to measure ^{95}Mo shifts at low temperatures corresponding to slow S inversion failed due to excessive

Table 7

^{95}Mo NMR parameters for complexes **1–6**

Complex	Chemical shift (δ) [a]	$\Delta\nu_{1/2}$ (Hz)
1	−1361.9	80
2	−1393.3	130
3	−1399.5	130
4	−1421.1	210
5	−1432.0	170
6	−1392.4	120

[a] Relative to aq. 2M Na_2MoO_4 (pH 11) at 20 °C.

line broadening of the signals. The chemical shifts at 20°C obtained for these complexes are to high frequency of those obtained for tetracarbonyl complexes of phosphorus, arsenic and antimony donor ligands (typically in the range −1550 to −1800 ppm) but to low frequency of signals obtained for nitrogen ligand complexes (−1050 to −1300 ppm) [8]. The chemical shifts are of similar magnitude to those obtained for the complexes $K[Mo(CO)_4(D_2COEt)]$, $Na[Mo(CO)_4(S_2CNR_2)]$ (R = Me, Et), $[NH_4][Mo(CO)_4\{S_2P(OEt)_2\}]$ and $K[Mo(CO)_4\{S_2C\overline{N(CH_2)_3CH_2}\}]$, which showed chemical shifts in the range −1380 to −1417 ppm [10].

The ^{95}Mo chemical shifts obtained for complexes **1–6** show interesting trends which may be related to the sulphur inversion barriers. Scrutiny of Table 7 reveals an increase in shielding of the ^{95}Mo nucleus in the order **1** < **2** < **3** < **4**, concomitant with a decrease in sulphur inversion barrier (and hence Mo–S bond strength). Although an inversion barrier was not calculated for **5**, previous evidence [3] suggests that the inversion barrier for this species should be even lower than that obtained for **4** as a result of the incorporation of unsaturation into the ligand backbone; the ^{95}Mo chemical shift obtained for **5** is therefore consistent with the overall trend. It is interesting to note that the chemical shift for the unsymmetrical ligand complex **6** is the average of the chemical shifts of the related symmetrical ligand complexes **1** and **4**. Similar trends in ^{95}Mo chemical shifts have been observed in the complexes [(arene$(Mo(CO)_3$] [9], where arene = toluene, *o*-, *m*- and *p*-xylene and mesitylene, where again increasing metal–ligand bond strengths correlated with deshielding of the ^{95}Mo nucleus [9].

Attempts to rationalise trends in ^{95}Mo and other transition metal NMR chemical shifts [8,18,19] are generally based on the Ramsey equation [20], which in its simplest form separates the overall shielding parameter σ into diamagnetic (σ^d) and paramagnetic (σ^p) components, hence

$$\sigma = \sigma^d + \sigma^p$$

For heavy nuclei such as ^{95}Mo, the paramagnetic term is the dominant factor influencing changes in nuclear shielding, and may be expressed [18] as

$$-\sigma^p = (2\mu_o/3\pi)\mu_B^2(\Delta E)^{-1}\left[\langle r^{-3}\rangle_p P_i + \langle r^{-3}\rangle_d D_i\right]$$

where r_p and r_d are the valence *p*- and *d*-electron radii respectively and P_i and D_i refer to the imbalance of *p* and *d* electrons around the nucleus. However, it has been shown that valence shell *p* contributions are unimportant for early transition metals [18], and the term $\langle r^{-3}\rangle_p P_i$ may be neglected in the following discussion. For transition metals the average excitation energy, ΔE, is essentially the ligand field splitting, Δ, or a weighted mean of the splittings for lower symmetries. This equation shows that deshielding is greater for small values of r_d and ΔE, and shielding of a nucleus such as ^{95}Mo will increase, for a given *d*-electron configuration, with an increase in ligand field strength and also with an increase in *d*-electron delocalisation, which decreases the radial factor $\langle r^{-3}\rangle_d$ [18].

Bearing these factors in mind, it is thus possible to attempt some rationalisation of the trends observed for the complexes **1–6**. Considering first the chemical shifts of the group as a whole relative to other Mo^0 complexes, the deshielding of the ^{95}Mo nucleus in compounds **1–6** relative to $Mo(CO)_6$ ($\delta \sim -1857$ ppm [19]) and related phosphine complexes of the type $[Mo(CO)_{6-n}(PR_3)_n]$ ($n = 1, 2$) [21] may be fully rationalised in terms of a reduction in overall ligand field strength (ΔE) on

replacing CO or PR_3 by a thioether ligand. The poor π-acceptor ability of the thioether ligands relative to CO or phosphine also reduces delocalisation of the *d*-electrons and is also a contributory factor towards the overall deshielding observed for complexes **1–6**.

Within the series of complexes **1–6**, the variations in chemical shift are most probably related to the localisation of *d*-electron density at the Mo centre. Weakening of the Mo–S bonding in a closely analogous series of complexes such as **1–6** would result in stronger metal–carbonyl bonding as a result of the reduced *trans*-influence of the dithioether. This in turn would induce increased π delocalisation of *d*-electrons into π^*(CO) orbitals, concomitantly decreasing $\langle r^{-3} \rangle_d$ and thus increasing nuclear shielding [19]. It is particularly interesting that the chemical shift observed for **6** is the average of that observed for **1** and **4**, indicating an additive influence of the individual ligating thioether sites on the overall ^{95}Mo chemical shift.

It is possible, therefore, to rationalise qualitatively the parallel trends observed in both sulphur inversion barriers and ^{95}Mo NMR chemical shifts for **1–6**. Similar correlations are to be expected between ^{53}Cr and ^{183}W chemical shifts and sulphur inversion barriers in the corresponding chromium and tungsten tetracarbonyl complexes, but these have not been reported to date because of the very low receptivities of these nuclei.

Acknowledgements

We thank the University of Exeter for a Studentship (to I.M.), and Dr. D. Stephenson for recording the 2D EXSY spectra.

References

1 D.A. Kleier and G. Binsch, J. Magn. Reson., 3 (1970) 146.
2 E.W. Abel, T.P.J. Coston, K.G. Orrell, V. Šik and D. Stephenson, J. Magn. Reson., 70 (1986) 34.
3 E.W. Abel, S.K. Bhargava and K.G. Orrell, Prog. Inorg. Chem., 32 (1984) 1, and ref. therein.
4 E.W. Abel, I. Moss, K.G. Orrell and V. Šik, J. Organomet. Chem., 326 (1987) 187.
5 E.W. Abel, I. Moss, K.G. Orrell, V. Šik and D. Stephenson, J. Chem. Soc., Dalton Trans., (1987) 2695.
6 E.W. Abel, I. Moss, K.G. Orrell, V. Šik, D. Stephenson, P.A. Bates and M.B. Hursthouse, J. Chem. Soc., Dalton Trans., (1988) 521.
7 P. Haake and P.C. Turley, J. Am. Chem. Soc., 89 (1967) 4617.
8 M. Minelli, J.H. Enemark, R.T.C. Brownlee, M.J. O'Connor and A.G. Wedd, Coord, Chem. Rev., 68 (1985) 169.
9 A.F. Masters, R.T.C. Brownlee, M.J. O'Connor and A.G. Wedd, Inorg. Chem., 20 (1981) 4183.
10 E.C. Alyea and A. Somogyvari, Inorg. Chim. Acta, 83 (1984) L49.
11 M.T. Ashby and D.L. Lichtenberger, Inorg. Chem., 24 (1985) 636.
12 D.F. Shriver, Manipulation of Air-Sensitive Compounds, McGraw-Hill, New York, 1969.
13 D. Welti and D. Whittaker, J. Chem. Soc., (1962) 4372.
14 H.C.E. Mannerskantz and G. Wilkinson, J. Chem. Soc., (1962) 4454.
15 G.R. Dobson, Inorg. Chem., 8 (1969) 90.
16 D.A. Kleier and G. Binsch, DNMR3 Program 165, Quantum Chemistry Exchange, Indiana University, 1970.
17 E.W. Ainscough, E.J. Birch and A.M. Brodie, Inorg. Chim. Acta, 20 (1976) 187.
18 J. Mason, Coord. Chem. Rev., 87 (1987) 1299, and ref. therein.
19 D. Rehder in J. Mason (Ed.), Multinuclear NMR, Chapt. 19, p. 499–504, Plenum Press, New York, 1987.
20 N.F. Ramsey, Phys. Rev., 77 (1950) 567.
21 P. Jaitner and W. Wohlgenannt, Monatsh. Chem., 113 (1982) 699.